

1 **Wild communities of *Morpho* butterflies reveal *Spiroplasma* endosymbiont with inflated**  
2 **genome size and peculiar evolution.**

3  
4 Jonathan Filée<sup>\*,1</sup>, Manuela López-Villavicencio<sup>2,6</sup>, Vincent Debat<sup>2,6</sup>, Rachel Fourdin<sup>7</sup>, Camilo  
5 Salazar<sup>3</sup>, Karina Lucas Silva-Brandão<sup>4</sup>, Patrick Blandin<sup>2</sup>, Andre Victor Lucci Freitas<sup>5</sup>, Carolina  
6 Pardo-Diaz<sup>3</sup> and Violaine Llaurens<sup>6,2</sup>

7  
8  
9 <sup>1</sup> Laboratoire Evolution, Génomes, Comportement, Ecologie, CNRS Université Paris-Saclay UMR9191, IRD  
10 UMR247, IDEEV, 12 route 128, 91198 Gif sur Yvette, France

11 <sup>2</sup> Institut de Systématique, Evolution et Biodiversité (UMR 7205 CNRS/MNHN/SU/EPHE/UA), Muséum National  
12 d'Histoire Naturelle - CP50, 45 rue Buffon, 75005 PARIS, France

13 <sup>3</sup> Department of Biology, Faculty of Natural Sciences, Universidad del Rosario. Carrera 24 # 63C-69, Bogota  
14 D.C., 111221, Colombia

15 <sup>4</sup> Leibniz Institute for the Analysis of Biodiversity Change, Museum of Nature Hamburg, Martin-Luther-King-Platz  
16 3, 20146 Hamburg, Germany

17 <sup>5</sup> Departamento de Biología Animal, Instituto de Biología, Universidade Estadual de Campinas, Campinas/SP,  
18 Brazil

19 <sup>6</sup> Centre Interdisciplinaire de Recherche en Biologie (UMR 7241 CNRS/INSERM/Collège de France) 11, place  
20 Marcelin Berthelot, 75005 Paris, France

21 <sup>7</sup> GeT-PlaGe, Bât G2, INRAE, 31326 Castanet-Tolosan Cedex, France

22  
23 \* Corresponding authors: E-mail: [jonathan.filee@universite-paris-saclay.fr](mailto:jonathan.filee@universite-paris-saclay.fr)

24  
25 **Keywords:** Lepidoptera, endosymbiont, toxin genes, speciation, insertion sequences

26  
27 **Abstract** (229 words)

28 The evolution of endosymbiont genomes is likely influenced by the ecological interactions with  
29 their hosts. Here, we studied the evolution of *Spiroplasma* genomes detected within *Morpho*  
30 butterflies sampled in the wild. *Spiroplasma* was detected in 4 out of the 11 *Morpho* species  
31 studied and displayed a 3 times larger genome size as compared to *Spiroplasma* genomes  
32 documented in other hosts. This inflation in genome size is caused by massive and recent  
33 expansion of various mobile genetic elements and by the acquisition of new genes stemming  
34 from prophages. In particular, we documented the peculiar evolution of the toxin genes in  
35 plasmids that may enhance host resistance to parasites. Phylogenetic comparisons with  
36 *Spiroplasma* extracted from other host point at a unique origin of *Spiroplasma* in *Morpho*, and  
37 strong divergence from *Spiroplasma* found in other Lepidoptera. Resequencing data obtained  
38 for multiple populations of the two sister-species *M. helenor* and *M. achilles* living in sympatry  
39 over the majority of their distribution revealed a opposite prevalence (97% in *M. achilles* and  
40 3% in *M. helenor*), suggesting contrasted ecological interactions with these two host-species.  
41 Reconciliation analysis of the phylogenetic relationships of *Morpho* mitochondrial genomes  
42 and *Spiroplasma* genomes was then consistent with a predominant vertical transfer of the  
43 endosymbiont. Altogether, our results suggest a key role of ecological interactions with the  
44 host in the evolution of endosymbiont genomes and point at a putative interaction of  
45 *Spiroplasma* with reproductive isolation between sympatric species of butterflies.

46  
47

## 48 Introduction

49

50 Ecological relationships between species generate selective pressures acting on their  
51 genomes. In turn, the evolution of genes in interacting species can modify their ecological  
52 interactions. Intracellular bacteria, or endosymbionts, offer the opportunity to investigate  
53 feedbacks between genome evolution and ecological interactions. Heritable microbial  
54 endosymbionts profoundly impact several life history traits of their hosts, affecting both their  
55 survival and reproductive success (Hurst 2017) as sex-ratio distortion (Harumoto and  
56 Lemaitre 2018) or protection against pathogens (Ballinger and Perlman 2019). They can  
57 therefore play a crucial role in population dynamics and diversification of the host species,  
58 especially when they induce cytoplasmic incompatibilities (Werren 1998). At the same time,  
59 the endosymbiont lifestyle is often associated with changes in its own genome (Wernegreen  
60 2017): the prevalence of genetic drift in endosymbiont populations and the hyper-  
61 specialization to their host induce fast and irreversible genome erosion and progressive loss  
62 of metabolic functions. The mutation accumulation and genome decay through Muller's  
63 ratchet is indeed documented as a specific feature of endosymbiotic bacteria (Moran 1996).  
64 Such reduction in the number of functional genes may in turn increase the extinction risk of  
65 endosymbiont populations (Bennett and Moran 2015), and as a consequence, symbiont  
66 replacement is commonly observed (Manzano-Marín et al. 2023). However, long-term  
67 persistence of some endosymbionts has also been documented, raising the question of how  
68 ecological interactions with the hosts limit genome decay (Naito and Pawlowska 2016).

69

70 Insect endosymbionts offer prominent examples of the diversity of ecological interactions  
71 (Drew et al. 2019), from positive effects as nutritional providers (Sudakaran et al. 2017) or  
72 protective agents against pathogens (Ballinger and Perlman 2019; King 2019) to negative  
73 ones acting as sex-ratio distorters or male-killing agents (Stevens et al. 2001). While the  
74 effects of endosymbionts on host survival and reproduction have been largely explored in  
75 insect model species like *Drosophila*, their prevalence and ecological impacts in wild  
76 communities are still largely unknown in most insects. Recent publications of large genomic  
77 datasets in insects now allow to better characterize the prevalence of these endosymbionts  
78 throughout arthropods (Medina et al. 2023) but, also, to investigate the evolution of these  
79 endosymbionts and the diversity of their ecological relationships with different hosts in the  
80 wild.

81

82 In Lepidoptera, the diversity and the impact of cytoplasmic endosymbionts on host  
83 phenotypes have been scarcely studied. *Spiroplasma* and *Wolbachia* are the most frequently  
84 reported endosymbionts, with various effects on host fitness (Duploux and Hornett 2018).  
85 Both produce male killing and sex ratio distortion in population of different Lepidoptera such  
86 as *Acraea encedon*, *Hypolimnas bolina* or *Danaus chrysippus* (Nymphalidae) (Duploux and  
87 Hornett 2018; Jiggins et al. 2000). However, the transmission of these endosymbionts across  
88 species is largely unknown, as well as the diversity of their impact on host phenotypes.

89

90 *Spiroplasma* are associated with a large variety of hosts, and their genomes appear highly  
91 eroded with reduced metabolic capacities, high proportion of pseudogenes, and elevated  
92 evolutionary rates (Gerth et al. 2021; Liu et al. 2022). In *Drosophila*, the prevalence of  
93 *Spiroplasma* among natural population is generally low (Watts et al. 2009; Haselkorn 2010),  
94 but in some cases, the fitness advantages brought to their hosts, such as protection against  
95 parasitic nematodes, can make it more common (Jaenike et al. 2010). Experimental infections  
96 show that *Spiroplasma* has high horizontal transmission efficiency (Nakayama et al. 2015) but

97 this ability is constrained by the phylogenetic distance between different hosts (Tinsley and  
98 Majerus 2007). However, *tempo* and patterns of *Spiroplasma* transmission in natural  
99 populations remain to be investigated. Therefore, studying the evolution of *Spiroplasma*  
100 genomes in natural populations of insects can now shed light on the feedbacks between  
101 bacterial genome evolution and ecological interactions with their hosts.

102  
103 Here, we focus on the *Spiroplasma* of nymphalid butterflies of the genus *Morpho* to  
104 characterize their level of ecological specialization, as well as their transmission mode. The  
105 genus *Morpho* is composed of emblematic species from the Neotropical rainforests, where up  
106 to ten different species can be observed in sympatry in Amazonian lowlands and the Guiana  
107 shield (Blandin and Purser 2013). Studying endosymbiont genomes found in *Morpho*  
108 butterflies from the wild allows to test (1) how much endosymbionts are shared across closely  
109 vs. distantly related host species, (2) how their genomes, and more specifically their toxin  
110 genes, evolved in different hosts, and (3) how endosymbionts are transmitted within and  
111 among sympatric host species. We used whole-genome sequencing data from 11 *Morpho*  
112 species to study the evolution of endosymbiont genomes in closely-related hosts. We then  
113 investigated the prevalence of endosymbionts in different populations of two sister-species of  
114 *Morpho* living in sympatry to characterize the transmission of the endosymbionts within and  
115 between species.

116

117

## 118 **Materials and Methods**

119

### 120 **Genus dataset**

121

122 To identify the diversity of endosymbiont genomes present in different *Morpho* species, we  
123 analyzed the sequencing data obtained using the PacBio HiFi methodology applied to  
124 specimens from 11 *Morpho* species: 9 Amazonian species (*M. marcus*, *M. eugenia*, *M.*  
125 *telemachus*, *M. hecuba*, *M. rhetenor*, *M. menelaus*, *M. deidamia*, *M. helenor*, *M. achilles*), and  
126 2 sympatric species ranging from western Ecuador to Central America (*M. amathonte*, *M.*  
127 *granadensis*). Note that within *M. telemachus* there are two sympatric morphs (with either  
128 blue or yellow wings), so we analyzed one individual per morph. This dataset including all  
129 sampled species is referred to as the *genus dataset*.

130

131 For each individual included in the *genus dataset*, the DNA extraction was carried out from  
132 the thorax muscles of a male individual using the Qiagen Genomic-tip 100/G kit, following  
133 supplier instructions. After DNA extraction, the sequencing library was prepared following the  
134 manufacturer's instructions "Procedure and Checklist Preparing HiFi SMRTbell Libraries  
135 Using SMRTbell Express Template Prep Kit 2.0." for *M. helenor*, *M. achilles* and *M. deidamia*  
136 and "Procedure and Checklist – Preparing whole genome and metagenome libraries using  
137 SMRTbell® prep kit 3.0" for the other species. Libraries were sequenced on several PacBio  
138 Sequel II SMRT cells with the adaptive loading method or by diffusion loading on a SequelII  
139 instrument (for additional details see (Bastide et al. 2023). The reads were assembled into  
140 contigs using Hifiasm (Cheng et al. 2021) using the option no purge (-I0) to avoid eventual  
141 over-purging symbiont sequences. The mitochondrial genome for all *Morpho* species was  
142 assembled directly from the PacBio Hifi reads with Rebaler  
143 (<https://github.com/rrwick/Rebaler>). For the assembly of mitochondrial genomes of *M.*  
144 *helenor*, *M. achilles* and *M. deidamia* the mitochondrial genome of the closely related

145 species *Pararge aegeria* was used as a reference (Bastide et al. 2023) while for the other  
146 eight species, we used the genome of *M. helenor* as a reference.

147

#### 148 *Endosymbiont metagenomic assembly*

149

150 To detect the presence of endosymbiont genomes in the *genus dataset*, we used  
151 Blobtools (Laetsch and Blaxter 2017) with Diamond as search engine (Buchfink et al. 2015)  
152 against the UniProt database using a local copy of the NCBI TaxID file for the taxonomic  
153 assignation of the best hits. Minimap2 (Li 2018) was used for read mapping with the options -  
154 ax map-hifi. Endosymbiont contigs were extracted using seqtk (available at  
155 <https://github.com/lh3/seqtk>) and processed through the Dfast workflow (Tanizawa et al.  
156 2018) to estimate statistics and taxonomic assignation. The completeness of the detected  
157 endosymbiont genomes was estimated with CheckM (Parks et al. 2015) with the  
158 corresponding gene sets. Endosymbiont genome annotations were carried out using  
159 PROKKA (Seemann 2014) with standard parameters, and the corresponding genetic codes.  
160 Whole genome alignments were created using the nucmer utility of the Mummer  
161 package (Marçais et al. 2018) with standard options. Structural variations were visualized  
162 using D-GENIES (Cabanettes and Klopp 2018).

163

#### 164 *Gene content in Spiroplasma genomes*

165

166 We aimed at distinguishing orthologous genes shared with previously published *Spiroplasma*  
167 genomes found in other hosts, from genes specific to *Spiroplasma* in *Morpho*. We  
168 downloaded a set of 62 *Spiroplasma* genome assemblies with comparable genome metrics  
169 (N50>100kb) from the NCBI Refseq Genomes FTP server 12/02/2022 version  
170 (<ftp://ftp.ncbi.nlm.nih.gov/genomes/refseq>). We used using Ortho-Finder 2.5.4 (Emms and  
171 Kelly 2015) to infer orthologous genes in the 62 *Spiroplasma* genomes as well as the *M.*  
172 *achilles* *Spiroplasma* genome sAch identified in this study. Then, functional annotation of the  
173 orthologous was inferred using the BlastKOALA tool against the KEGG database (Kanehisa  
174 et al. 2016).

175

176 We then studied putative toxin genes either implied in host-protective phenotypes or host  
177 male killing in insects. We used the HMMER software (Mistry et al. 2013) seeded with protein  
178 sequences of each symbiont genome and the Pfam domain sequence alignments (Finn et al.  
179 2014) corresponding to the OTU (PF02338 and OTU-like cysteine protease) and RIP  
180 (PF00161) as databases. Domain architectures of all matching proteins were then computed  
181 using PfamScan (Mistry et al. 2007) and SIGNALP 6.0 (Teufel et al. 2022). Phylogenies of the  
182 toxin proteins were built by extracting and aligning the corresponding OTU domains. The  
183 phylogenetic trees were inferred using IQ-TREE v2.1.3 (Nguyen et al. 2015) by estimating the  
184 best substitution models using ModelFinder (Kalyaanamoorthy et al. 2017). Branch support  
185 was then assessed by performing 1000 replicates using UltraFast bootstraps (Hoang et al.  
186 2018).

187

188

#### 189 *Phylogeny of Spiroplasma*

190

191 A previously published set of 96 single-copy, non-recombinant orthologs from the  
192 *Spiroplasma* genomes (Gerth et al. 2021) was used to assess the phylogenetic relationships  
193 of these endosymbionts. Orthologs were identified using the best reciprocal BLASTP hits of

194 each of the 96 protein sequences using the *Spiroplasma poulsonii* sMel gene sequences as  
195 seeds and lead to a dataset of 72 gene sequences present in all of the *Morpho Spiroplasma*  
196 genomes. Alignments were computed using MAFFT (Kato et al. 2002) and manually  
197 corrected to exclude ambiguous regions and taxa with sequence similarity >99% were  
198 removed. Phylogenetic analyses were carried out using IQ-TREE v2.1.3 (Nguyen et al. 2015),  
199 and genes were partitioned to estimate the best substitution models using ModelFinder  
200 (Kalyaanamoorthy et al. 2017). Branches supports were assessed by performing 1000  
201 replicates using UltraFast bootstraps (Hoang et al. 2018). The resulting trees were rooted  
202 using the *Spiroplasma* sequences belonging to the *ixodetis* clade in accordance with the  
203 literature.

204

205

### 206 *Prediction of mobile genetic elements in Spiroplasma genomes*

207

208 Inserted sequences (ISs) were identified by querying the ISFinder database (Siguier et al.  
209 2006) with protein sequences of each endosymbiont genome assemblies using BLAST with  
210 *e-value*  $\leq 10e-10$  (Altschul et al. 1990).

211 Plasmid sequences were identified using the Plasflow software (Krawczyk et al. 2018) and  
212 prophage regions were found using two methods: (1) a sequence-similarity search using  
213 PHASTER (Arndt et al. 2016), and (2) a *de novo* prediction using PhiSpy (Akhter et al. 2012).  
214 Predictions gathered from the two methods were then merged in a single file. Comparative  
215 genomics with other prokaryotic genomes were then computed using a set of 25,674 genome  
216 sequences with comparable genome metrics (N50>100kb) downloaded from the NCBI  
217 Refseq Genomes FTP server 12/02/2022 version (<ftp://ftp.ncbi.nlm.nih.gov/genomes/refseq>).  
218 The corresponding proteomes were then downloaded and ISs were identified using the same  
219 procedure as described above for *Morpho* endosymbionts (using the 62 *Spiroplasma*  
220 genomes for which plasmids and phage regions were identified with the same previous  
221 workflow).

222

### 223 **Sister-species dataset**

224

225 To study vertical and horizontal transmission of *Spiroplasma*, we focused on multiple  
226 populations of *M. achilles* and *M. helenor*, two sister-species living in sympatry across most of  
227 their distribution (Blandin and Purser 2013). We analyzed re-sequencing data obtained from  
228 43 males of *M. helenor* and 33 individuals (20 males and 3 females) of *M. achilles*  
229 (Supplementary Table 1). This second dataset is referred to as the *sister-species dataset*.

230

### 231 *DNA extractions and genome sequencing of M. helenor and M. achilles*

232

233 For the *sister-species dataset*, DNA for each individual was extracted from thorax muscle  
234 using the DNeasy Blood & Tissue Kit following the producer instructions. In most cases, DNA  
235 was extracted from SNAP-frozen individuals or samples preserved in DMSO, but we also  
236 used 13 samples of dried pinned *M. achilles* from the personal collection of Patrick Blandin  
237 (Supplementary Table 1).

238

239 Sequencing was then performed at the GeT-PlaGe core facility of INRAE. DNA-seq libraries  
240 were prepared using the Illumina TruSeq Nano DNA LT Library Prep Kit, following supplier  
241 instructions. Briefly, DNA was fragmented by sonication and adaptors were ligated. Eight  
242 cycles of PCR were then applied to amplify libraries. Library quality was assessed using an

243 Advanced Analytical Fragment Analyzer and quantified by QPCR using the Kapa Library  
244 Quantification Kit. Sequencing was performed on an Illumina Novaseq 6000, using a paired-  
245 end read length of 2x150 pb on a S4 Flowcell.

246

#### 247 *Population genomics of Spiroplasma in the sister-species dataset*

248

249 Adaptors were removed from the reads with cutadapt (Martin 2011) and the reads of each  
250 individual were mapped against the original *Spiroplasma* genome found in the reference  
251 genome of *M. achilles* (referred to as *sAch* hereafter) using BWA-mem v0.7.17 (Li 2013).  
252 Then we used Samtools v1.10 (Li et al. 2009) to sort the resulting SAM and BAM files and  
253 recover the fasta sequences from *Spiroplasma* endosymbionts, which were then assembled  
254 using Megahit (Li et al. 2015) with default parameters. To assess the presence/absence of  
255 *Spiroplasma* in each individual, we blasted each contig against the *sAch* genome using  
256 BLASTN with e-value cutoff =  $10e-50$  and identity percentage  $>90\%$ . Matching contigs were  
257 extracted and the presence/absence of the endosymbiont in a sample was classified as  
258 follows: (i) 'presence' when more than 100kb of aligned matching contigs were obtained, (ii)  
259 'ambiguous' when 5-100kb of aligned contigs were obtained, (iii) 'absence' when less than  
260 5kb of aligned sequences were obtained. To validate this classification, we identified the 16S  
261 rDNA gene from each sample using BLASTN against the 16S rDNA gene from the reference  
262 genome *sAch*, with e-value cutoff of  $10e-50$  and identity percentage  $>90\%$ . Then, we  
263 estimated a phylogenetic tree for *Spiroplasma* using the 16S rDNA sequences retrieved from  
264 the different butterfly samples, following the same procedure stated earlier, and using the  
265 *Spiroplasma mellifera* KC3 sequence (NCBI accession CP029202) as outgroup.

266

267 Finally, RIP/Spaid toxin genes were also retrieved from each butterfly sample by applying a  
268 TBLASTN using the RIP/Spaid toxin gene identified in the *sAch* genome as seed, with e-  
269 value cutoff =  $10e-10$ .

270

#### 271 *Tree reconciliation analysis in order to predict host lateral switches*

272

273 *Spiroplasma*, as maternally transmitted endosymbionts, are inherited together with the  
274 mitochondrial genome of the host. Therefore, we used ecceTERA (Jacox et al. 2016) to  
275 reconcile the mtDNA phylogeny of *Morpho* with the *Spiroplasma* 16S rDNA phylogeny  
276 previously obtained, and for which identical sequences were removed to eliminate tree  
277 polytomies. SylvX (Chevenet et al. 2016) was used to visualize and interpret the reconciliation  
278 tree.

279

280 The *Morpho* phylogeny was estimated with whole mitochondrial genomes, for which we  
281 combined those obtained in the genus-dataset and the sister-species datasets. Mitochondrial  
282 genomes for all individuals in the sister-species dataset were extracted directly from Illumina  
283 reads with GetOrganelle v1.7.5.3 (Jin et al. 2020) and the parameters -R 10 -k  
284 21,45,65,85,105 -F animal\_mt. Alignments were generated using MAFFT (Katoh et al. 2002)  
285 and manually curated to exclude ambiguous regions. The phylogeny was obtained with IQ-  
286 TREE v2.1.3 (Nguyen et al. 2015), estimating the best substitution model with ModelFinder  
287 (Kalyaanamoorthy et al. 2017), and assessing branch support with 1000 UltraFast bootstrap  
288 replicates (Hoang et al. 2018). We used the *Heliconius melpomene* sequence (NCBI  
289 accession HE579083) as outgroup.

290

291

## 292 Results

### 293 294 *Morpho* butterflies are sporadically associated with *Spiroplasma* symbionts

295  
296 We sequenced and surveyed genomes of 11 species of *Morpho* butterflies (including two  
297 different morphs of *M. telemachus*), for the presence of endosymbiotic bacteria (so-called  
298 *genus dataset*). Contigs were binned using their GC%, read coverage and taxonomic  
299 assignment (Figure 1). The resulting blob-plots indicate the presence of a limited number of  
300 symbionts: the genomes of *M. achilles*, *M. amathonte* and *M. rhetenor* had contigs with very  
301 low GC% that match with *Spiroplasma*, whereas the genomes of *M. hecuba* and *M. helenor*  
302 had contigs associated with *Wolbachia* and *Enterococcus*. In contrast, the genomes of the  
303 remaining six species of *Morpho* (i.e. *M. marcus*, *M. eugenia*, *M. telemachus*, *M. menelaus*,  
304 *M. deidamia* and *M. granadensis*) do not seem to harbor symbiont sequences  
305 (Supplementary Figure 1).

306  
307 We recovered and assembled three *Spiroplasma* genomes (*sAma*, *sAch* and *sRhe*) from the  
308 genomes of *M. amathonte*, *M. achilles* and *M. rhetenor*, respectively. The *sAch* assembly was  
309 the most complete, containing 98% of a set of lineage-specific, single-copy, *Spiroplasma*  
310 marker genes (Table 1). The other two (*sAma* and *sRhe*) had lower completeness (60% and  
311 78%, respectively, Table 1), indicating that only a fraction of the corresponding genomes was  
312 captured.

313  
314  
315 **Table 1. Assembly statistics of the endosymbiont genomes identified in genomes of *Morpho* butterflies**

Name	Host	Taxonomic assignment	Size (kb)	N50 (kb)	Completeness (%)	Contigs (#)	Coding ratio (%)	GC (%)
sAch	<i>M. achilles</i>	<i>Spiroplasma</i> sp.	4075	2667	98	46	46	24
sAma	<i>M. amathonte</i>	<i>Spiroplasma</i> sp.	3144	2570	60	16	45	24
sRhe	<i>M. rhetenor</i>	<i>Spiroplasma</i> sp.	2860	157	78	44	46	24
wHec	<i>M. hecuba</i>	<i>Wolbachia</i>	1444	1444	100	1	84	34
eHel	<i>M. helenor</i>	<i>Enterococcus faecalis</i>	4618	2787	100	38	86	36

### 316 317 318 *Inflation of genome size of Spiroplasma found in Morpho butterflies*

319  
320 The assemblies of *Spiroplasma* retrieved from *Morpho* genomes display a considerable larger  
321 genome size (2,9Mb to 4,1Mb) than the 62 previously-published genomes of this  
322 endosymbiont (1.1 Mb to 1.9 Mb; Supplementary Figure 2). The *sAch* and *sAma* assemblies  
323 contained a large contig of 2,7 Mb and 2,5 Mb, respectively, with low levels of synteny  
324 (Supplementary Figure 3). The *sAch* and *sAma* assemblies were also composed of 46 and 15  
325 small contigs ranging from 17kb to 74kb, while the assembly of *sRhe* is composed of 44  
326 contigs ranging from 14kb to 320kb (Figure 1). The 46 small contigs of the *sAch* assembly fall  
327 into 4 clusters based on sequence alignments, but all of them differ in size and/or in  
328 nucleotide similarity (Supplementary Figure 3).

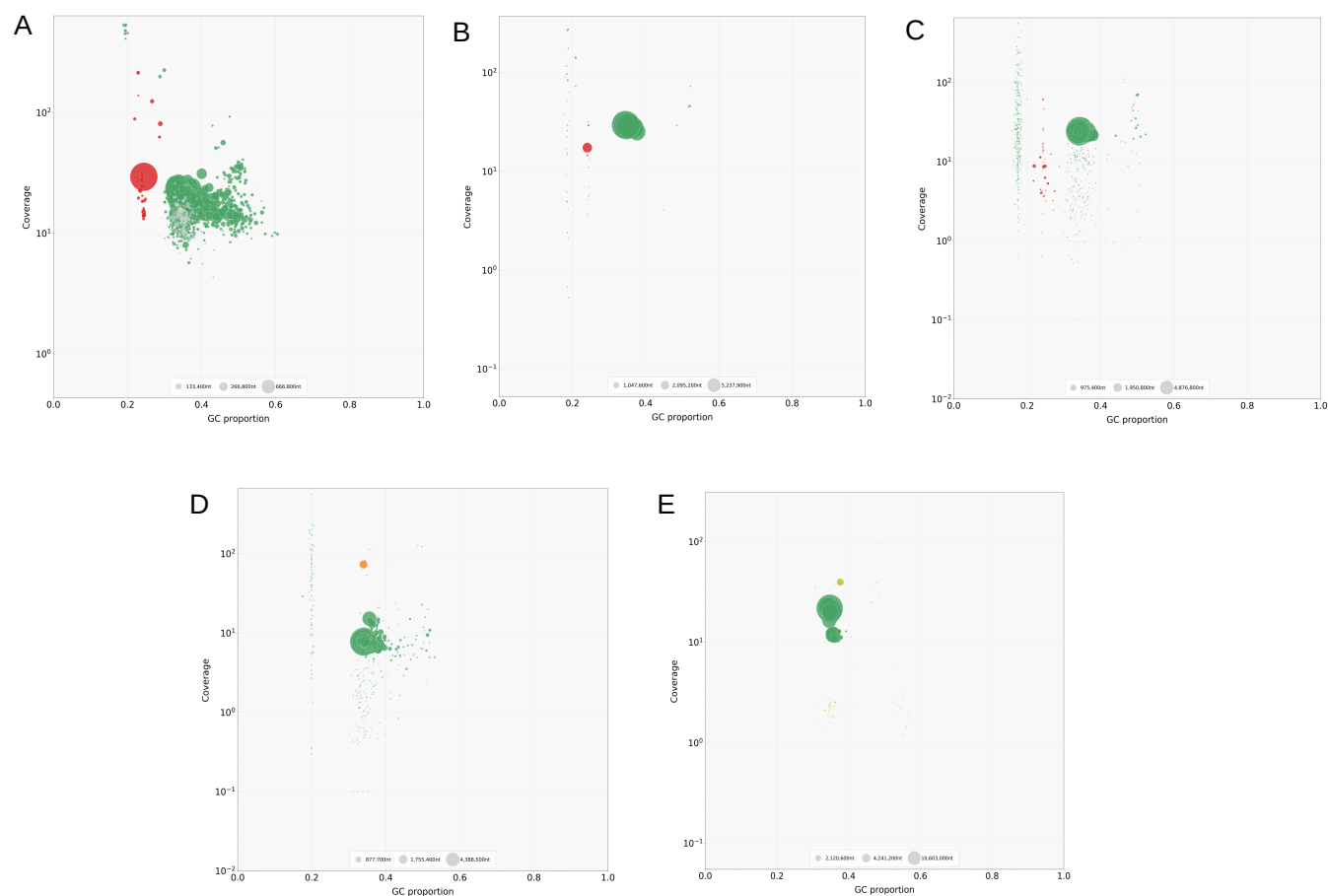
329 To assess how much new genes contributed to the expansion of genome size in the  
330 *Spiroplasma* associated with *Morpho*, we searched for orthologous genes in *sAch*, which is  
331 the most complete assembly. Similar to other *Spiroplasma*, *sAch* contains a number of  
332 conserved orthologous group of genes that ranges from 600 to 1000 ortho-groups, but has an  
333 unusually large number of species-specific genes (>350 singletons; Supplementary Figure 4).

334  
335

336 *Spiroplasma* found in *Morpho* are divergent from *Spiroplasma* in other *Lepidoptera*

337

338 To investigate the evolutionary origin of the *Spiroplasma* detected in *Morpho*, we built a  
339 phylogeny of this endosymbiont using a set of 72 concatenated single copy genes present in  
340 all *Spiroplasma* genomes available in the database, with recognizable homologs in the sAch  
341 complete genome. The assemblies sAma, sAch and sRhe retrieved from *Morpho* were  
342 monophyletic and are included within the *citri* clade (Figure 2), which includes diverse plant  
343 pathogens and endosymbionts of insects such as Hemiptera (*Spiroplasma kunkelli*), Diptera  
344 (*S. sp. sNigra*) and Hymenoptera (*S. melliferum*). The 16S rDNA phylogeny that includes a  
345 broader taxonomic dataset confirms this observation (Supplementary Figure 6). Intriguingly,  
346 the *Spiroplasma* recovered from *Morpho* are highly divergent from those found in other  
347 Lepidoptera such as the moth *Homona magnanima* (*S. ixodetis* sHM) or the nymphalid  
348 butterfly *Danaus chrysippus* (*S. sp. Danaus chrysippus*), both in the *ixodetis* clade (Figure 2) .



350 **Figure 1: Detection of symbionts within genomic sequences of *Morpho*: *M. achilles* (A), *M. amathonte***  
351 **(B), *M. rhetenor* (C), *M. hecuba* (D) and *M. helenor* (E).** Contigs represented as circles were binned based on  
352 their GC%, read coverage, and taxonomic assignment. Dark green contigs matched arthropod sequences, red  
353 contigs matched Mollicutes (*Spiroplasma*), orange contigs matched Proteobacteria (*Wolbachia*), and light green  
354 contigs matched Firmicutes (*Enterococcus*). The size of the circle is proportional to the size of the contigs.

355

356

357

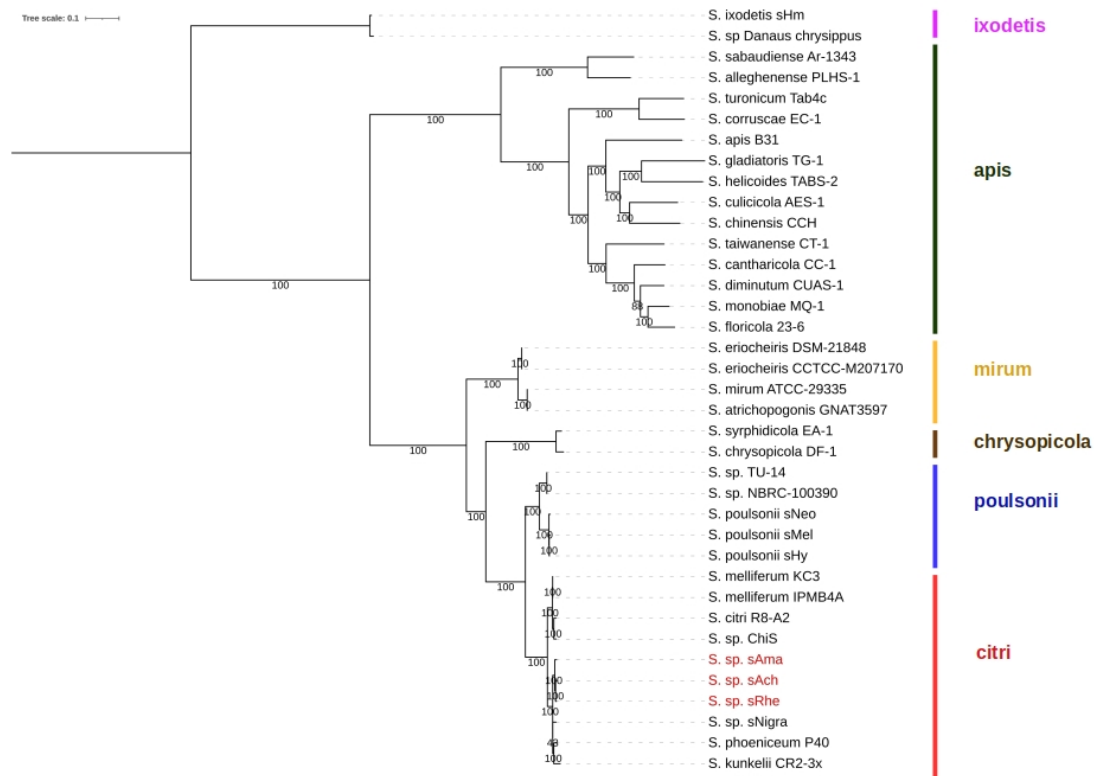
358

359

360



361  
362



363 **Figure 2: Phylogenetic reconstruction of *Spiroplasma* from different hosts based on the conserved set**  
 364 **of 72 single copy orthologous genes.** Recognized *Spiroplasma* clades are indicated in colors (right), and the  
 365 *Spiroplasma* detected in *M. amathonte*, *M. achilles* and *M. rhetenor* (sAma, sAch and sRhe, respectively) are  
 366 highlighted in red. Phylogeny was constructed using 1000 bootstrap replicates. The phylogeny made with an  
 367 extended gene dataset of 96 orthologs including only sAch produces the same topology (Supplementary Figure  
 368 5). Note that the *Spiroplasma* documented in other Lepidoptera (the butterfly *Danaus chrysippus* and the moth  
 369 *Homona magnanima*) fall in the distantly-related ixodetis clade (pink).

370

371

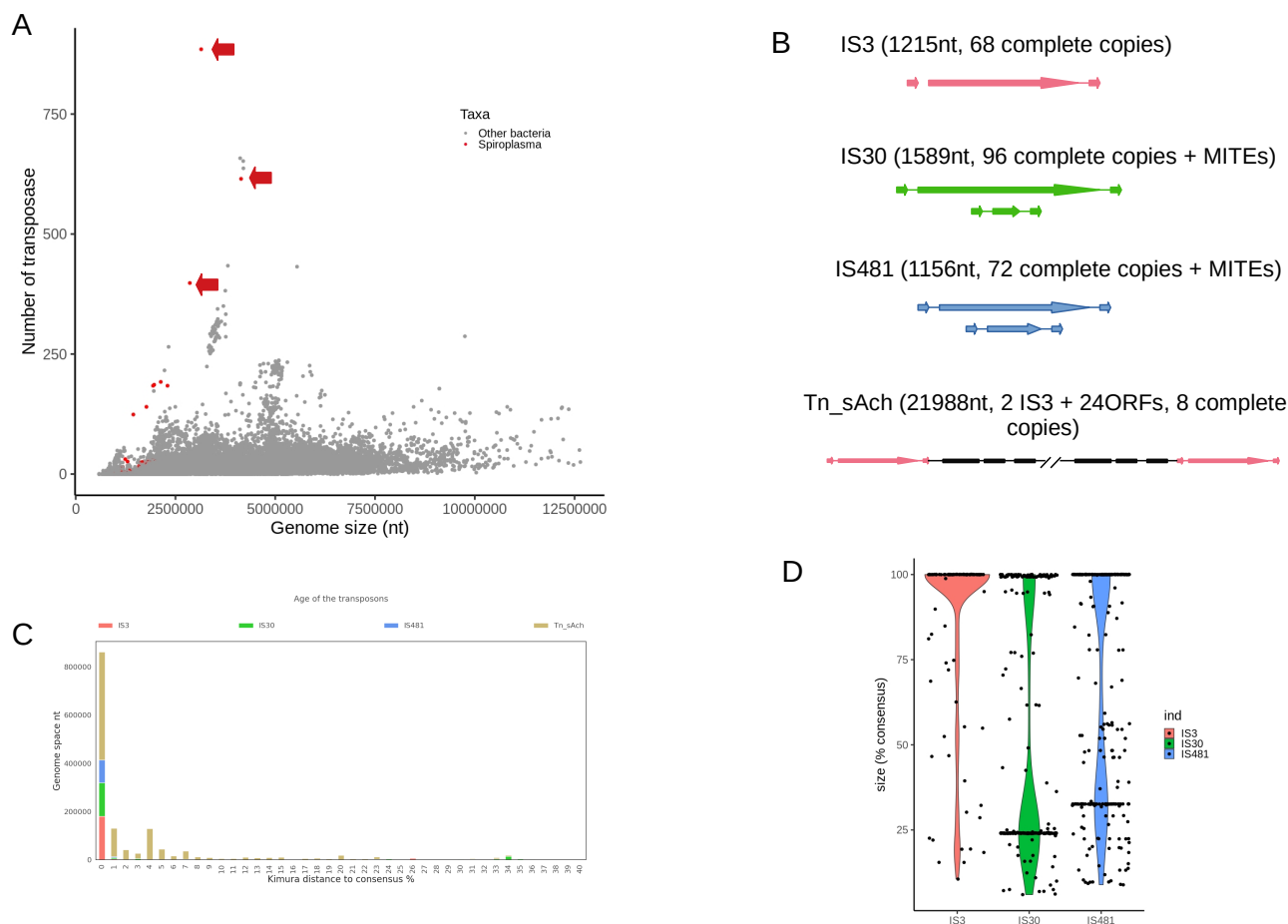
372 *Proliferation of mobile genetic elements in Spiroplasma found in Morpho*

373

374 We found multiple mobile genetic elements (i.e., prokaryotic transposons, ISs, plasmids and  
 375 prophages) integrated in the large genomes of the *Spiroplasma* retrieved from *Morpho*. We  
 376 observed that ISs are unusually abundant in these endosymbiont genomes, reaching a  
 377 record-level in prokaryotes, that ranges from 398 to 885 copies (Figure 3A). The sAch  
 378 assembly suggests this proliferation is associated with a surprisingly low number of IS  
 379 families (Figure 3B). Indeed, only four IS families have expanded: an IS3-like family with 68  
 380 complete copies, an IS30 family with 96 complete copies, and a IS481 family with 72 intact  
 381 copies. The fourth group is a 22kb composite transposon that we named Tn\_sAch. This  
 382 transposon has two IS3 copies at the tips and 24 conserved ORFs in the middle. In the  
 383 assembly sAch, we observed Tn\_sAch elements being especially common in the small  
 384 contigs (constituting ~54% of their length) and much less frequent in the large 2,7Mb contig  
 385 (accounting for only 9% of its length). The strong structural conservation of the backbone of  
 386 the 8 intact copies of Tn\_sAch suggests *en bloc* successive transpositions in the genome.

387 Sequence similarities of the different transposon copies analyzed as a proxy of the age of the  
 388 different transposition events, indicates that most of them are identical or nearly identical,  
 389 suggesting very recent transpositions (Figure 3C), but the copies of Tn\_sAch have higher  
 390 sequence divergence suggesting the presence of older copies.

391 The IS30 and IS481 transposons have generated non-autonomous Miniature Inverted repeat  
 392 Transposable Elements (MITEs) by internal deletion leading to smaller transposons that  
 393 represent 25% and 32% of the size of the parental elements (Figure 3D). In contrast, most of  
 394 the complete autonomous IS copies are 100% full-length and presumably intact, showing few  
 395 truncated copies. Such high level of complete and identical IS copies strongly suggests that  
 396 these families have recently expanded in the genomes of the *Spiroplasma* found in *Morpho*.  
 397



399 **Figure 3: Insertion Sequences (ISs) found in the genomes of *Spiroplasma* found in *Morpho*.** **A:** Number of  
 400 transposase encoding genes found in a set of 25,675 prokaryotic genomes that include 62 *Spiroplasma*  
 401 genomes (red dots) and three *Morpho Spiroplasma* (red dots with arrows) plotted against their genome sizes. **B:**  
 402 Structure of the IS families found in the complete sAch genome and their main properties. Each colors represent  
 403 a distinct IS families, arrows correspond to transposase genes and their internally deleted derivatives (MITEs),  
 404 black rectangles indicate passenger genes of the composite transposon. **C:** Analysis of the age of the IS  
 405 copies in the sAch genome using the Kimura 2-parameter distance between the consensus sequence of a given  
 406 family and all the individual copies that compose the family. The results are ordered based on the total amount of  
 407 nucleotides. **D:** Analysis of the completeness of the different IS copies found in the sAch genome estimated as  
 408 the percentage of the total length of the corresponding consensus sequences.

410 Our analyses of phage sequence invasion reveal the 28 to 32 integrated prophages in the  
 411 genomes of *Spiroplasma* in *Morpho*, accounting for 418 kb in sAma, 482 kb in sRhe, and 538

412 kb in sAch (Supplementary Figure 7). The density of phage-derived elements (7.8/Mb) is thus  
413 larger than that in the most prophage-rich bacterial genome known to date (6.9/Mb),  
414 (Touchon et al. 2016; Frost et al. 2020). Interestingly, more than 80% of the sAch species-  
415 specific genes (singletons) are located in phage regions (Supplementary Figure 4). Functional  
416 analysis of these genes indicated that they are enriched by two KEGG functional categories:  
417 “genetic information processing” and “signaling and cellular processes” (Supplementary  
418 Figure 4). Therefore, the genome size expansion in *Spiroplasma* of *M. achilles* is associated  
419 with the accumulation of new genes acquired through interactions with phages.

420

421 Furthermore, the sAch, sAma and sRhe assemblies encode for six, four and five different  
422 plasmids respectively. They are all characterized by substantial higher level of read coverage  
423 than the genome contigs (Figure 1) suggesting the presence of multiple identical copies per  
424 bacterial cells.

425

426

427 *Toxin genes identified in the Spiroplasma genomes of healthy Morpho males*

428

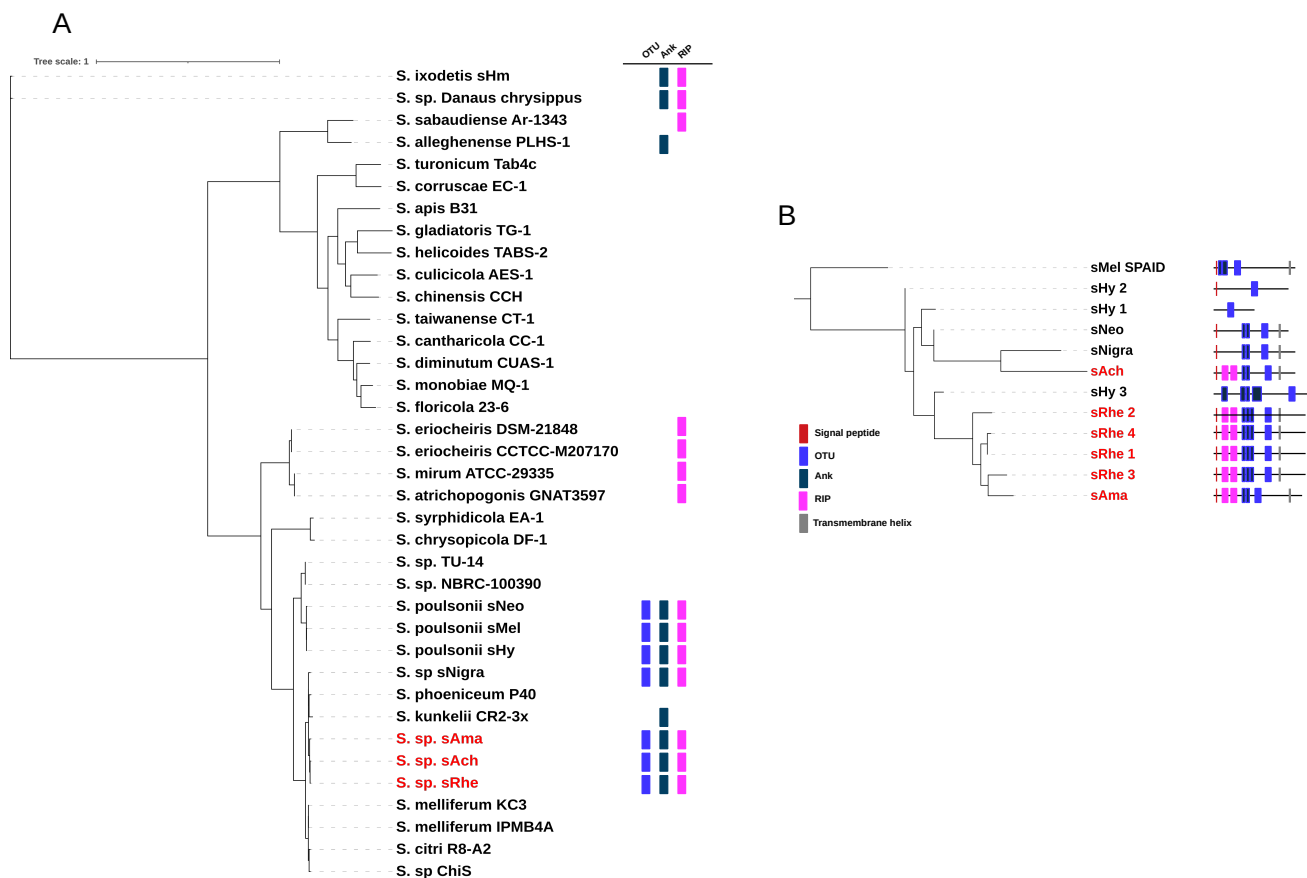
429 As insects *Spiroplasma* are known to induce striking phenotypes in their host, such as male-  
430 killing promoted by the Spaid toxin or protection against parasites (RIP-like enzyme)  
431 (Harumoto and Lemaitre 2018; Ballinger and Perlman 2019), we specifically searched for  
432 these genes. One of the plasmids detected in both the sAch and sAma assemblies encodes  
433 for an ORF that combines both a RIP locus and a complete and structurally conserved Spaid  
434 gene (Figure 4B). This apparent bi-functional gene encodes for two RIP proteins in the 5' end  
435 and a Spaid protein in 3' end. The latter includes both ankyrin repeats (Ank) and a  
436 deubiquitinase domain (OTU), which are known to occur in the *Spiroplasma* strain sMel  
437 (Figure 4B) and induce male-killing in *Drosophila melanogaster* embryo. We sporadically  
438 observed ankyrin repeats, the OTU domain, and RIP domains in other genomes of  
439 *Spiroplasma* (Figure 4A). In particular, four homologous copies of RIP/OTU/Ank domains  
440 were also present in the sRhe assembly, and all of them are located on four different contigs.  
441 Although RIP-encoding genes are present in various *Spiroplasma* genomes (Figure 4A), the  
442 fusion of the RIP domain with the Spaid domain is an original feature found in all of the  
443 *Morpho Spiroplasma* genomes (Figure 4B). These features open the possibility that  
444 *Spiroplasma* endosymbionts may induce some peculiar phenotype in their *Morpho* butterfly  
445 hosts.

446

447

448

449



451 **Figure 4: Distribution and organization of the toxin genes found in genomes of *Spiroplasma*.** **A:**  
 452 Distribution of the OTU (blue), Ankyrin (grey) and RIP (fuchsia) encoding domains across the *Spiroplasma* whole-  
 453 genome phylogeny. **B.** Phylogeny based on the OTU domain alignment of the Spaid-like proteins. Domain  
 454 prediction based on Pfam similarity with known domains. The position of the *Morpho Spiroplasma* is highlighted  
 455 in red in both trees.

456

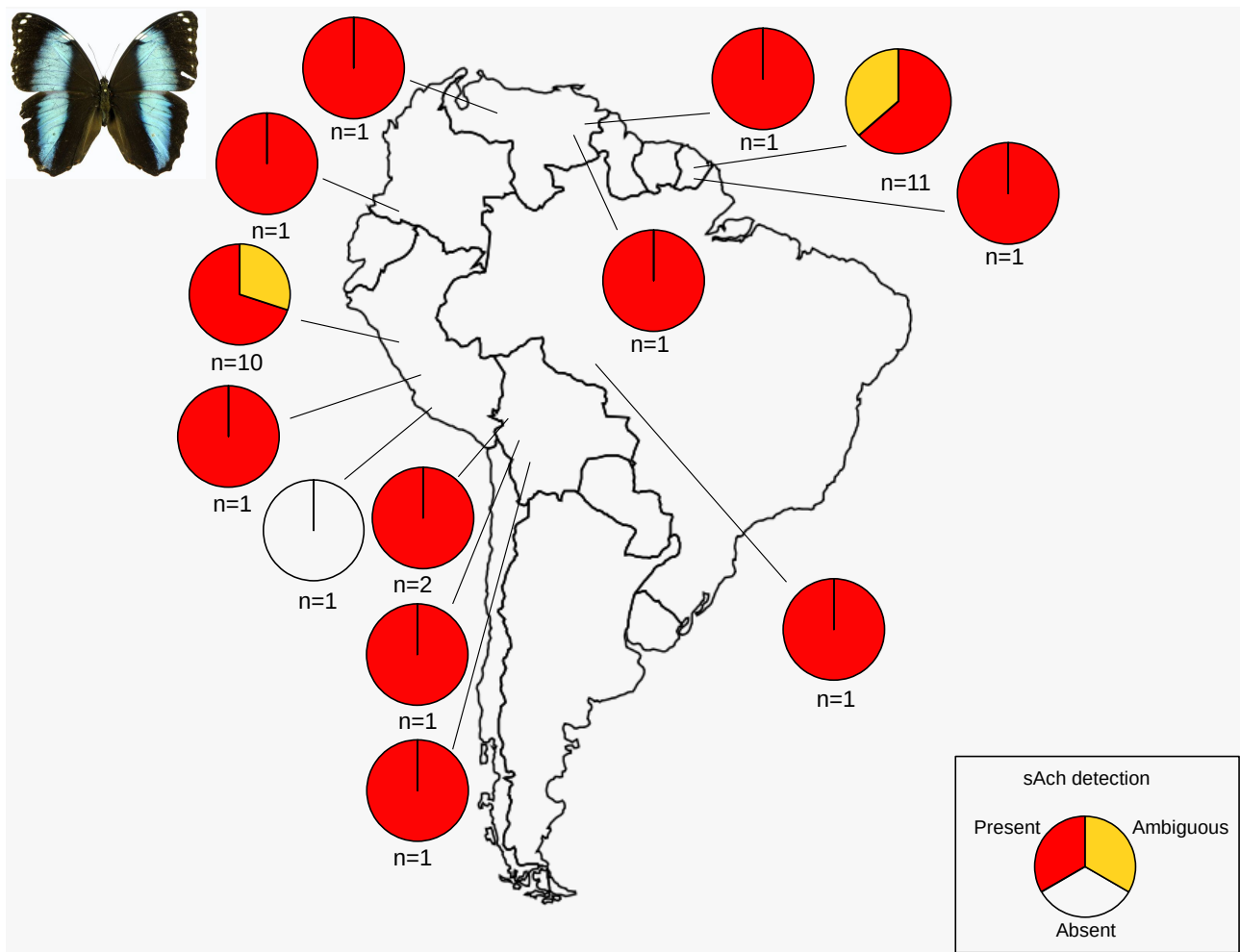
#### 457 *Horizontal and vertical transfer of Spiroplasma in Morpho*

458

459 To estimate the prevalence of *Spiroplasma* within species of *Morpho* and test for horizontal  
 460 vs. vertical transfer of this endosymbionts, we searched for the presence of *Spiroplasma* in  
 461 different populations of *M. achilles* and its sister and sympatric species *M. helenor*. We  
 462 detected genomes of *Spiroplasma* with assembly size >100 kb and highly matching the sAch  
 463 assembly in 26 out of 33 individuals of *M. achilles*; only 6 individuals had few contigs  
 464 matching sAch (with assembly size <100kb), and a single one lacked any genomic trace of it  
 465 (Figure 5 and Supplementary Table 1). Thus, all populations of *M. achilles* accross south-  
 466 America had *Spiroplasma*, except for one population in Peru represented by a single  
 467 individual in our study (Figure 5). By contrast, among the 43 *M. helenor* individuals from 27  
 468 populations we investigated, only a single individual had *Spiroplasma*. Therefore, although *M.*  
 469 *achilles* and *M. helenor* are sympatric species throughout the Amazonian basin and are  
 470 closely-related species (3,6 millions years of divergence (Chazot et al. 2021), they display  
 471 completely opposite patterns of infection by *Spiroplasma*.

472

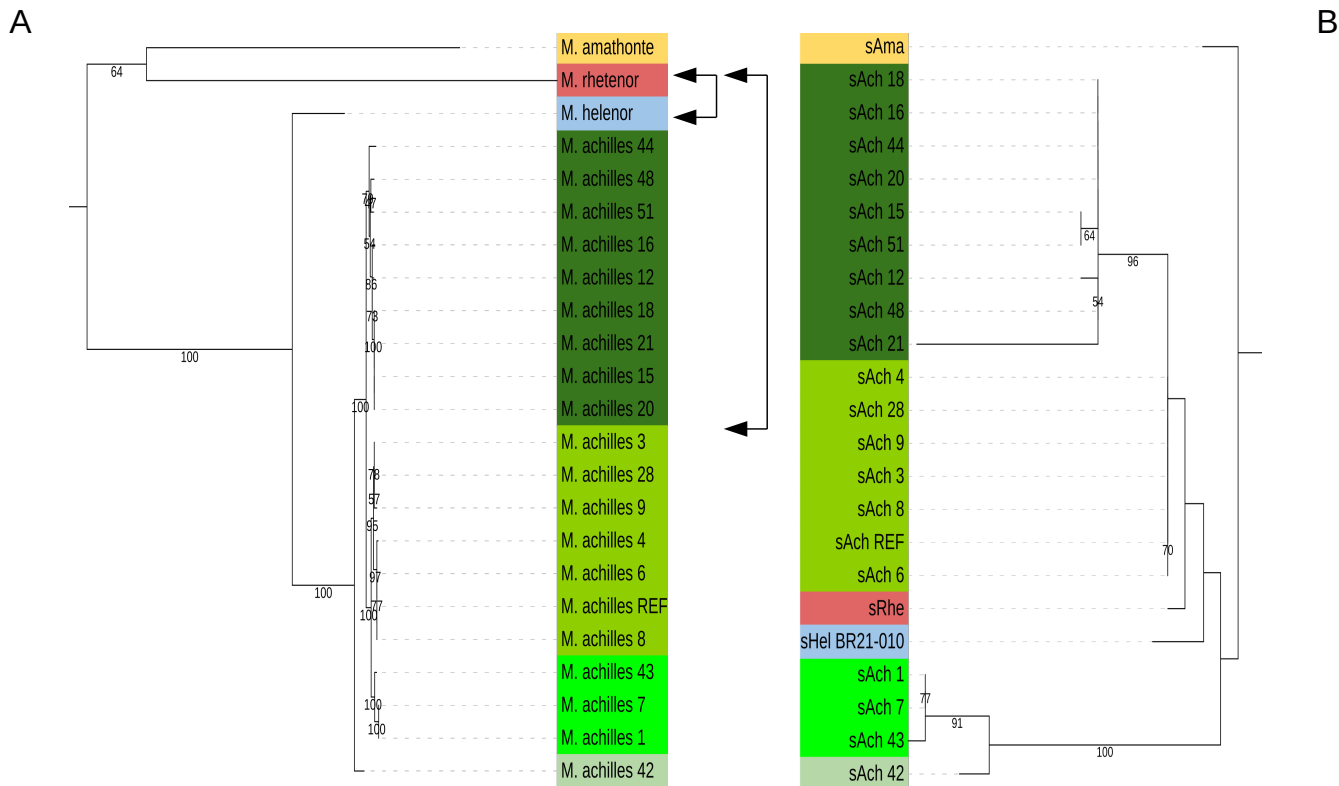
473



474 **Figure 5: Geographic distribution of *Spiroplasma* in populations of *Morpho achilles*.** Each circle  
475 represents a population of *M. achilles* and the number of individuals sampled per population is indicated on the  
476 bottom. The presence of *Spiroplasma* in each population is color coded as red (presence), yellow (ambiguous)  
477 and white (absence). See also Supplementary Figure 8.  
478  
479

480 Most of the *Spiroplasma* identified here had large genome assemblies (>1 Mb) albeit the use  
481 of short-read sequencing technology that generally failed to assemble highly repeated  
482 regions. Moreover, some assemblies reached sizes comparable to the reference sAch  
483 assembly (>3 Mb; Supplementary Figure 8). The 16S rDNA gene was present in most of  
484 these *Spiroplasma* assemblies, and homologous RIP and Spaid toxin genes were also found  
485 almost universally (Supplementary Figure 8). In the 16s rDNA phylogeny, the only  
486 *Spiroplasma* genome retrieved from *M. helenor* and the sRhe *Spiroplasma* from *M. rhetenor*  
487 both appear well nested into the sAch clades from *M. achilles* (Figure 6 and Supplementary  
488 Figure 8). This suggests a putative horizontal transmission of *Spiroplasma* between *M.*  
489 *helenor*, *M. achilles* and *M. rhetenor* living in sympatry. The reconciliation analysis between  
490 the *Spiroplasma* tree (16S rDNA) and the *Morpho* tree (whole mitochondrial genomes) are  
491 highly congruent suggesting that both the endosymbiont and mtDNA are maternally inherited  
492 (Figure 6), except for sHel and sRhe. This finding strongly suggests lateral exchange of  
493 *Spiroplasma* between *M. achilles*, *M. rhetenor* and *M. helenor* (Figure 6). The high  
494 congruence between the *Spiroplasma* and the mitochondrial tree within *M. achilles* agrees  
495 with a predominant vertical maternal transmission.

496



497 **Figure 6: Reconciliation analysis between the host tree (A) contrasted against the endosymbiont tree (B)**  
 498 **with predicted horizontal host switches of *Morpho Spiroplasma*.** Whole mitochondrial genome tree for  
 499 *Morpho* against the 16S rDNA tree for *Spiroplasma*. Ultra-fast bootstraps values are indicated on each branch.  
 500 Color blocs correspond to the main phylogenetic clusters identified in the species phylogeny. Double-arrows  
 501 highlight the possible horizontal host switches.  
 502  
 503

504

## 504 Discussion

505

### 506 Peculiar evolution of *Spiroplasma* genomes in *Morpho* butterflies

507

508 We documented the presence of the bacterial endosymbiont *Spiroplasma* in four out of 11  
 509 species of *Morpho* butterflies studied here, highlighting that the association with this  
 510 endosymbiont greatly varies across closely related host species, even when they live in  
 511 sympatry. Surprisingly, the genomes of *Spiroplasma* retrieved from *Morpho* sharply differ from  
 512 those in other Lepidoptera, suggesting horizontal transfer among distantly-related host  
 513 species. The phylogenetic discrepancies between *Spiroplasma* genes and mitochondrial  
 514 genes across *Morpho* species also suggests that horizontal transfer between species living in  
 515 sympatry might occur. The circulation of *Spiroplasma* in the hemolymph is thought to facilitate  
 516 horizontal transfer across sympatric species, for instance through the consumption of  
 517 hemolymph by mites (Jaenike et al. 2010). Because the *Spiroplasma* found in *Morpho*  
 518 butterflies is closely related to strain documented as a plant pathogen, the inter-specific  
 519 transmission of this symbionts could also be enabled by the shared consumption of host  
 520 plants by caterpillars. Remarkably, the three *Morpho* species presenting close *Spiroplasma*  
 521 (*M. achilles*, *M. helenor* and *M. rhetenor*) share several hostplants in French Guyana,  
 522 supporting this hypothesis (Anon 2017). The presence of *Spiroplasma* in *Morpho* butterflies  
 523 might thus stem from interactions with other insects or through host plant consumption.

524 However, population genomics of *Spiroplasma* within the species *M. achilles* species indicate  
525 widespread distribution and predominance of vertical transmission at the species level.  
526 Interestingly, we have evidenced the presence of *Spiroplasma* symbiont in *M. amathonte* and  
527 *M. achilles*, two species that have diverged from more than 17 My (Chazot et al. 2021) and  
528 that currently occupying non-overlapping geographical ranges: *M. amathonte* is found in  
529 central America and in the western slopes of the Andes while *M. achilles* inhabits the  
530 Amazonian basin. The weak genome synteny of the *Spiroplasma* genomes of these two  
531 species and the congruence of host and symbiont phylogenies support a vertical transmission  
532 from a common ancestor. Thus, the ubiquitous presence of *Spiroplasma* in *M. achilles*  
533 populations across south-America and the predominant vertical transmission of the symbiont  
534 at various evolutionary time-scale point at a long-term association between *Spiroplasma*  
535 symbiont and *Morpho* butterflies. The absence of *Spiroplasma* from some *Morpho* species  
536 (e.g. *M. menelaus*, closely related to *M. amathonte*) would then suggest a secondary loss.

537  
538 *Massive genome size promoted by large expansion in diverse mobile genetic elements.*

539  
540 While endosymbionts as *Spiroplasma* display streamlined genomes (Gerth et al. 2021), the  
541 genome size of the *Spiroplasma* observed in our study is surprisingly large. Our analyses  
542 indicate that recent and massive expansion of diverse mobile genetic elements (MGE) are  
543 responsible for this striking inflation in genome size. Record-level of Insertion Sequences  
544 (accounting for 1550 kb), integrated prophages (538kb) and plasmids (278 kb) represent  
545 nearly 60% of the total genome size of the *Spiroplasma* found in *M. achilles* (accounting for  
546 2366 kb on a total genome size of 4075 kb). All *Spiroplasma* genomes detected in *Morpho*  
547 butterflies display such extreme expansion of MGE, in sharp contrast with the paucity of MGE  
548 generally found in *Spiroplasma* (Gerth et al. 2021) or *Wolbachia* genomes (Cerveau et al.  
549 2011). Moreover, most of the IS copies found in *Spiroplasma* of *Morpho* butterflies are  
550 recently-transposed elements, indicating an ongoing and continuous accumulation. Such  
551 MGE proliferation has also been sporadically observed in *Orientia* symbionts, a widespread  
552 *Rickettsia*-like, intra-cellular bacteria associated with mites (Batty et al. 2018) and in  
553 *Mycoplasma* endosymbionts, associated with diverse fungi (Naito and Pawlowska 2016). In  
554 addition, integrated phage genomes provide numerous new genes and functions in  
555 *Spiroplasma* associated with *Morpho* butterflies. The massive expansion of MGEs leads to an  
556 inflated genome size but also provides a source of new genes and functions expanding the  
557 diversity of the genomic repertoire of *Spiroplasma* symbionts infecting *Morpho* butterflies.

558 Recombination induced by MGEs and the gene flow provided by phage genome integration  
559 can explain the lack of genome erosion in the *Spiroplasma* of *Morpho*, that contrasts with the  
560 important genome size reduction observed in most endosymbionts. Such rapid evolution  
561 might stem from peculiar adaptation in the symbionts of *Morpho*, allowing long-term  
562 association and high prevalence in some *Morpho* species. For instance, MGE-encoded toxin  
563 genes might have contributed to increase the symbiont persistence in some *Morpho* butterfly  
564 populations.

565  
566 *Evolution of toxin genes and putative protective effect*

567  
568 By detecting *Spiroplasma* in adult *Morpho* males sampled in the wild, our study suggests that  
569 the presence of *Spiroplasma* does not prevent the development of males in *Morpho*  
570 butterflies, in sharp discrepancy with the male-killing effects reported in the butterfly *Danaus*  
571 *chrysippus* (Jiggins et al. 2000), but similar to the results obtained with *Wolbachia* in  
572 Neotropical Acraeini (Nymphalidae) (Silva-Brandão et al. 2021). More specifically, the toxin

573 gene *Spaid* found in *Spiroplasma poulsonii* and documented to trigger male killing in  
574 *Drosophila* (Harumoto and Lemaitre 2018) does not have the male-killing (MK) effect in  
575 *Morpho*. It is thus possible that *Morpho* butterflies have developed resistance to the sex-ratio  
576 distortion effect of the *Spiroplasma Spaid* toxins. Such MK-suppression have indeed been  
577 observed in plant-hopper (Yoshida et al. 2021) and in lacewing (Hayashi et al. 2018).  
578 Alternatively, as *Spaid* toxins target the gene dosage compensation system that increases the  
579 transcription of genes on the male single X chromosome in *Drosophila* (Harumoto & Lemaitre  
580 2018), it is also possible that this toxin is ineffective in ZW sex-determination system for which  
581 the female is heterogametic. Supporting this view, MK-inducing *Spiroplasma* in Lepidoptera  
582 lack the *Spaid* toxins genes, but the genetic determinant(s) of the MK phenotype are unknown  
583 (Arai et al. 2022). However, strong conservation of the *Spaid* genes among *Morpho* species  
584 and populations favors the idea that it provides a selective advantage.  
585 Interestingly, our study also reveals the evolution of specific architecture of toxin genes in the  
586 *Spiroplasma* of *Morpho* butterflies, including *RIP* physical linkage with the *Spaid* gene. While  
587 the functional implication of this evolution cannot be inferred from our current results, the high  
588 conservation of this specific architecture in the *Morpho* genomes is consistent with an  
589 adaptive role. Moreover, the localization of these genes on plasmids also suggests that they  
590 may spread across bacteria, and their persistence might have been promoted by natural  
591 selection, either because they act as selfish elements or because of positive impact on host  
592 fitness. In *Drosophila*, *RIP* proteins produced by *Spiroplasma poulsonii* have indeed been  
593 documented to induce positive effects on host survival, through their protective effect against  
594 nematodes (Stevens et al. 2001), as well as parasitoid wasps (Ballinger and Perlman 2019).  
595 Such defensive effect of *Spiroplasma* could have a positive impact on the fitness of *Morpho*  
596 butterflies and might explain their high prevalence in *M. achilles*.

597  
598 *Contrasted prevalence of Spiroplasma in sympatric sister species: do Spiroplasma impact*  
599 *reproductive isolation?*

600  
601 The evolution of the *Spaid* gene might have resulted in a change of function in *Morpho*  
602 butterflies, disabling the male-killing mechanism. Alternatively, resistance to male-killing effect  
603 might have evolved in *Morpho* butterflies. The evolution of MK-suppression has been  
604 documented in natural populations of the butterfly *Hypolimnys bolina* (Nymphalidae) infected  
605 by *Wolbachia* (Hornett et al. 2022). Such evolution of resistance is likely to be under strong  
606 positive selection given the high fitness costs for the hosts induced by male-killing genes  
607 (Hornett et al. 2022). The *Spiroplasma* is highly prevalent in *M. achilles* and quite rare in the  
608 sympatric species *M. helenor* despite the similarity of the *Spaid* gene in both species, this  
609 might suggest that resistance to the deleterious effect of *Spiroplasma* could be restricted to  
610 *M. achilles*.

611 Alternatively, the presence of the symbiont might trigger cytoplasmic incompatibilities (CI),  
612 explaining the huge difference in its prevalence between these two sister-species living in  
613 sympatry. *Spiroplasma*-induced cytoplasmic incompatibilities have been recently documented  
614 in the wasp *Lariophagus distinguendus* (Pollmann et al. 2022). In case of CI, crosses  
615 between infected males and uninfected females generally do not produce offspring; CI could  
616 thus limit genetic exchange between the two sympatric species.

617 Altogether, our current results on the contrasted *Spiroplasma* prevalence in these sister-  
618 species therefore raises the question of the potential impact of this endosymbiont as barrier to  
619 gene flow between these sympatric species. Endosymbionts like *Spiroplasma* and *Wolbachia*  
620 have indeed been suggested to generate post-zygotic barriers to gene flow (see (Duplouy  
621 and Hornett 2018) for a review), but their role in initiating vs. reinforcing speciation remains



622 largely uncovered. Our study therefore points at the needs to investigate the effect of  
623 *Spiroplasma* on reproductive isolation and its significance for species diversification and co-  
624 existence in sympatry.

625

## 626 **Conclusion**

627

628 Studies on heritable symbionts in natural populations generally support a dynamic model of  
629 gene gain and loss shaped by the ecological interactions with their host. On the other hand,  
630 heritable symbiont lifestyle induces genetic isolation and population bottlenecks that lead to  
631 mutational decay and genome streamlining. In comparison with *Spiroplasma* genomes  
632 retrieved from other insects, *Morpho Spiroplasma* genomes display a massive expansion of  
633 diverse mobile genetic elements as transposable elements, prophages or plasmids. In  
634 addition, we documented a strong conservation of toxin RIP and Spaid-encoding genes in the  
635 *Spiroplasma* of *Morpho* species, that might enhance protection of the butterflies against  
636 parasites. The study of *Spiroplasma* symbionts in natural population of diverse *Morpho*  
637 butterfly species support a stable association in *Morpho achilles* populations across south-  
638 America, whereas *Spiroplasma* appears almost absent in sympatric *M. helenor* populations.  
639 This contrasted symbiont distribution among sympatric *Morpho* species is associated with a  
640 global predominant vertical transmission of the symbiont supporting a model in which the  
641 symbiont provides fitness advantages to the butterfly. Indeed, *Morpho Spiroplasma* genomes  
642 display a remarkable resistance to genome erosion by the mean of massive expansions of  
643 diverse mobile genetic elements as transposable elements, prophages or plasmids. In  
644 addition, the strong conservation of toxin RIP and Spaid-encoding genes might be the key-  
645 drivers of this lasting association either by conferring host protection against parasite and/or  
646 by limiting hybridization with symbiont-free sympatric *Morpho* species. Our study calls for  
647 additional investigations of the phenotypic effects of the *Spiroplasma* on their butterfly hosts  
648 to better understand how their ecological interactions shapes – and is shaped by – their  
649 evolution.

650

## 651 **Acknowledgments**

652

653 We would like to thank Heloïse Bastide and David Ogereau for their helps at the initial phase  
654 of this work, Josephine Ledamoisel, Rémi Mauxion and Owen MacMillan for their support  
655 during fieldwork in Panama, as well as Mathieu Chouteau and Mélanie McClure during  
656 fieldwork in Peru and French Guiana. Some of the analyses and simulations were performed  
657 on the the Plateforme de Calcul Intensif et Algorithmique PCIA (MNHN/CNRS), on the MeSU  
658 platform at Sorbonne-Université and on the Genotoul bioinformatics platform Toulouse  
659 Occitanie (Bioinfo Genotoul).

660

## 661 **Data Availability**

662

663 PacBio (*genus dataset*) and Illumina (*sister-species dataset*) read sequences and genome  
664 assemblies generated in this study were deposited in the NCBI database under the  
665 bioprojects PRJNA1069011 and PRJNA1063620. Primary raw data for each analysis can be  
666 downloaded at <https://doi.org/10.6084/m9.figshare.24582867.v1>

667

668

669

670

671

## 672 **Funding**

673

674 This work was supported by the European Research Council (ERC) Consolidator Grant  
675 101088089 “OUTOFTHEBLUE”, the ANR-tremplin and the CNRS MITI project ECODEMO.

676

## 677 **References**

678

Akhter S, Aziz RK, Edwards RA. 2012. PhiSpy: a novel algorithm for finding prophages in bacterial genomes that combines similarity- and composition-based strategies. *Nucleic Acids Research* 40:e126.

Altschul SF, Gish W, Miller W, Myers EW, Lipman DJ. 1990. Basic local alignment search tool. *J. Mol. Biol.* 215:403–410.

Anon. 2017. Les Morpho – Distribution, diversification, comportement - Les Lépidoptéristes de France. Available from: <https://www.lepidofrance.fr/monographies/morpho-distribution-diversification-comportement/>

Arai H, Inoue MN, Kageyama D. 2022. Male-killing mechanisms vary between *Spiroplasma* species. *Frontiers in Microbiology* [Internet] 13. Available from: <https://www.frontiersin.org/journals/microbiology/articles/10.3389/fmicb.2022.1075199>

Arndt D, Grant JR, Marcu A, Sajed T, Pon A, Liang Y, Wishart DS. 2016. PHASTER: a better, faster version of the PHAST phage search tool. *Nucleic Acids Research* 44:W16–W21.  
Ballinger MJ, Perlman SJ. 2019. The defensive *Spiroplasma*. *Current Opinion in Insect Science* 32:36–41.

Bastide H, López-Villavicencio M, Ogereau D, Lledo J, Dutrillaux A-M, Debat V, Llaurens V. 2023. Genome assembly of 3 Amazonian Morpho butterfly species reveals Z-chromosome rearrangements between closely related species living in sympatry. *GigaScience* 12:giad033.

Batty EM, Chaemchuen S, Blacksell S, Richards AL, Paris D, Bowden R, Chan C, Lachumanan R, Day N, Donnelly P, et al. 2018. Long-read whole genome sequencing and comparative analysis of six strains of the human pathogen *Orientia tsutsugamushi*. *PLOS Neglected Tropical Diseases* 12:e0006566.

Bennett GM, Moran NA. 2015. Heritable symbiosis: The advantages and perils of an evolutionary rabbit hole. *Proceedings of the National Academy of Sciences* 112:10169–10176.

Blandin P, Purser B. 2013. Evolution and diversification of Neotropical butterflies: Insights from the biogeography and phylogeny of the genus *Morpho* Fabricius, 1807 (Nymphalidae: Morphinae), with a review of the geodynamics of South America. *Tropical Lepidoptera Research*:62–85.

Buchfink B, Xie C, Huson DH. 2015. Fast and sensitive protein alignment using DIAMOND. *Nat Methods* 12:59–60.

- Cabanettes F, Klopp C. 2018. D-GENIES: dot plot large genomes in an interactive, efficient and simple way. *PeerJ* 6:e4958.
- Cerveau N, Leclercq S, Leroy E, Bouchon D, Cordaux R. 2011. Short- and Long-term Evolutionary Dynamics of Bacterial Insertion Sequences: Insights from Wolbachia Endosymbionts. *Genome Biology and Evolution* 3:1175–1186.
- Chazot N, Blandin P, Debat V, Elias M, Condamine FL. 2021. Punctuational ecological changes rather than global factors drive species diversification and the evolution of wing phenotypes in Morpho butterflies. *Journal of Evolutionary Biology* 34:1592–1607.
- Cheng H, Concepcion GT, Feng X, Zhang H, Li H. 2021. Haplotype-resolved de novo assembly using phased assembly graphs with hifiasm. *Nat Methods* 18:170–175.
- Chevenet F, Doyon J-P, Scornavacca C, Jacox E, Jousselein E, Berry V. 2016. SylvX: a viewer for phylogenetic tree reconciliations. *Bioinformatics* 32:608–610.
- Drew GC, Frost CL, Hurst GD. 2019. Reproductive Parasitism and Positive Fitness Effects of Heritable Microbes. In: *Encyclopedia of Life Sciences*. 1st ed. Wiley. p. 1–8. Available from: <https://onlinelibrary.wiley.com/doi/10.1002/9780470015902.a0028327>
- Duploux A, Hornett EA. 2018. Uncovering the hidden players in Lepidoptera biology: the heritable microbial endosymbionts. *PeerJ* 6:e4629.
- Emms DM, Kelly S. 2015. OrthoFinder: solving fundamental biases in whole genome comparisons dramatically improves orthogroup inference accuracy. *Genome Biology* 16:157.
- Finn RD, Bateman A, Clements J, Coggill P, Eberhardt RY, Eddy SR, Heger A, Hetherington K, Holm L, Mistry J, et al. 2014. Pfam: the protein families database. *Nucleic Acids Research* 42:D222–D230.
- Frost CL, Siozios S, Nadal-Jimenez P, Brockhurst MA, King KC, Darby AC, Hurst GDD. 2020. The Hypercomplex Genome of an Insect Reproductive Parasite Highlights the Importance of Lateral Gene Transfer in Symbiont Biology. *mBio* 11:10.1128/mbio.02590-19.
- Gerth M, Martinez-Montoya H, Ramirez P, Masson F, Griffin JS, Aramayo R, Siozios S, Lemaitre B, Mateos M, Hurst GDD. 2021. Rapid molecular evolution of Spiroplasma symbionts of Drosophila. *Microbial Genomics* [Internet] 7. Available from: <https://www.ncbi.nlm.nih.gov/pmc/articles/PMC8208695/>
- Harumoto T, Lemaitre B. 2018. Male-killing toxin in a bacterial symbiont of Drosophila. *Nature* 557:252–255.
- Haselkorn TS. 2010. The Spiroplasma heritable bacterial endosymbiont of Drosophila. *Fly* 4:80–87.

- Hayashi M, Nomura M, Kageyama D. 2018. Rapid comeback of males: evolution of male-killer suppression in a green lacewing population. *Proceedings of the Royal Society B: Biological Sciences* 285:20180369.
- Hoang DT, Chernomor O, von Haeseler A, Minh BQ, Vinh LS. 2018. UFBoot2: Improving the Ultrafast Bootstrap Approximation. *Molecular Biology and Evolution* 35:518–522.
- Hornett EA, Kageyama D, Hurst GDD. 2022. Sex determination systems as the interface between male-killing bacteria and their hosts. *Proceedings of the Royal Society B: Biological Sciences* 289:20212781.
- Hurst GDD. 2017. Extended genomes: symbiosis and evolution. *Interface Focus* 7:20170001.
- Jacox E, Chauve C, Szöllősi GJ, Ponty Y, Scornavacca C. 2016. ecceTERA: comprehensive gene tree-species tree reconciliation using parsimony. *Bioinformatics* 32:2056–2058.
- Jaenike J, Unckless R, Cockburn SN, Boelio LM, Perlman SJ. 2010. Adaptation via Symbiosis: Recent Spread of a *Drosophila* Defensive Symbiont. *Science* 329:212–215.
- Jiggins FM, Hurst GDD, Jiggins CD, Schulenburg JHG v d, Majerus MEN. 2000. The butterfly *Danaus chrysippus* is infected by a male-killing *Spiroplasma* bacterium. *Parasitology* 120:439–446.
- Jin J-J, Yu W-B, Yang J-B, Song Y, dePamphilis CW, Yi T-S, Li D-Z. 2020. GetOrganelle: a fast and versatile toolkit for accurate de novo assembly of organelle genomes. *Genome Biol* 21:241.
- Kalyaanamoorthy S, Minh BQ, Wong TKF, von Haeseler A, Jermini LS. 2017. ModelFinder: fast model selection for accurate phylogenetic estimates. *Nat Methods* 14:587–589.
- Kanehisa M, Sato Y, Morishima K. 2016. BlastKOALA and GhostKOALA: KEGG Tools for Functional Characterization of Genome and Metagenome Sequences. *Journal of Molecular Biology* 428:726–731.
- Katoh K, Misawa K, Kuma K, Miyata T. 2002. MAFFT: a novel method for rapid multiple sequence alignment based on fast Fourier transform. *Nucleic Acids Res.* 30:3059–3066.
- King KC. 2019. Defensive symbionts. *Curr Biol* 29:R78–R80.
- Krawczyk PS, Lipinski L, Dziembowski A. 2018. PlasFlow: predicting plasmid sequences in metagenomic data using genome signatures. *Nucleic Acids Research* 46:e35.
- Laetsch DR, Blaxter ML. 2017. BlobTools: Interrogation of genome assemblies. Available from: <https://f1000research.com/articles/6-1287>
- Li D, Liu C-M, Luo R, Sadakane K, Lam T-W. 2015. MEGAHIT: an ultra-fast single-node solution for large and complex metagenomics assembly via succinct de Bruijn graph. *Bioinformatics* 31:1674–1676.

Li H. 2013. Aligning sequence reads, clone sequences and assembly contigs with BWA-MEM. Available from: <http://arxiv.org/abs/1303.3997>

Li H. 2018. Minimap2: pairwise alignment for nucleotide sequences. *Bioinformatics* 34:3094–3100.

Li H, Handsaker B, Wysoker A, Fennell T, Ruan J, Homer N, Marth G, Abecasis G, Durbin R, 1000 Genome Project Data Processing Subgroup. 2009. The Sequence Alignment/Map format and SAMtools. *Bioinformatics* 25:2078–2079.

Liu P, Li Yuxin, Ye Y, Chen J, Li R, Zhang Q, Li Yuan, Wang W, Meng Q, Ou J, et al. 2022. The genome and antigen proteome analysis of *Spiroplasma mirum*. *Frontiers in Microbiology* [Internet] 13. Available from: <https://www.frontiersin.org/journals/microbiology/articles/10.3389/fmicb.2022.996938>

Manzano-Marín A, Coeur d'acier A, Clamens A-L, Cruaud C, Barbe V, Jousset E. 2023. Co-obligate symbioses have repeatedly evolved across aphids, but partner identity and nutritional contributions vary across lineages. *Peer Community Journal* [Internet] 3. Available from: <https://peercommunityjournal.org/articles/10.24072/pcjournal.278/>

Marçais G, Delcher AL, Phillippy AM, Coston R, Salzberg SL, Zimin A. 2018. MUMmer4: A fast and versatile genome alignment system. *PLOS Computational Biology* 14:e1005944.

Martin M. 2011. Cutadapt removes adapter sequences from high-throughput sequencing reads. *EMBnet.journal* 17:10–12.

Medina P, Russell SL, Corbett-Detig R. 2023. Deep data mining reveals variable abundance and distribution of microbial reproductive manipulators within and among diverse host species. *PLOS ONE* 18:e0288261.

Mistry J, Bateman A, Finn RD. 2007. Predicting active site residue annotations in the Pfam database. *BMC Bioinformatics* 8:298.

Mistry J, Finn RD, Eddy SR, Bateman A, Punta M. 2013. Challenges in homology search: HMMER3 and convergent evolution of coiled-coil regions. *Nucleic Acids Research* 41:e121.

Moran NA. 1996. Accelerated evolution and Muller's ratchet in endosymbiotic bacteria. *Proceedings of the National Academy of Sciences* 93:2873–2878.

Naito M, Pawlowska TE. 2016. Defying Muller's Ratchet: Ancient Heritable Endobacteria Escape Extinction through Retention of Recombination and Genome Plasticity. *mBio* 7:10.1128/mbio.02057-15.

Nakayama S, Parratt SR, Hutchence KJ, Lewis Z, Price T a. R, Hurst GDD. 2015. Can maternally inherited endosymbionts adapt to a novel host? Direct costs of *Spiroplasma* infection, but not vertical transmission efficiency, evolve rapidly after horizontal transfer into *D. melanogaster*. *Heredity* 114:539–543.

Nguyen L-T, Schmidt HA, von Haeseler A, Minh BQ. 2015. IQ-TREE: A Fast and Effective Stochastic Algorithm for Estimating Maximum-Likelihood Phylogenies. *Molecular Biology and Evolution* 32:268–274.

Parks DH, Imelfort M, Skennerton CT, Hugenholtz P, Tyson GW. 2015. CheckM: assessing the quality of microbial genomes recovered from isolates, single cells, and metagenomes. *Genome Res.* 25:1043–1055.

Pollmann M, Moore LD, Krimmer E, D'Alvise P, Hasselmann M, Perlman SJ, Ballinger MJ, Steidle JLM, Gottlieb Y. 2022. Highly transmissible cytoplasmic incompatibility by the extracellular insect symbiont *Spiroplasma*. *iScience* 25:104335.

Seemann T. 2014. Prokka: rapid prokaryotic genome annotation. *Bioinformatics* 30:2068–2069.

Siguier P, Perochon J, Lestrade L, Mahillon J, Chandler M. 2006. ISfinder: the reference centre for bacterial insertion sequences. *Nucleic Acids Res.* 34:D32-36.

Silva-Brandão KL, Cirino M, Magaldi LDM, Gueratto PE, Mattos RG, Freitas AVL. 2021. Subspecies limits and hidden *Wolbachia* diversity in *Actinote pellenea* butterflies. *Systematics and Biodiversity* 19:1012–1025.

STEVENS L, GIORDANO R, FIALHO RF. 2001. Male-killing, nematode infections, bacteriophage infection, and virulence of cytoplasmic bacteria in the genus *Wolbachia*. *Annu. rev. ecol. syst* 32:519–545.

Sudakaran S, Kost C, Kaltenpoth M. 2017. Symbiont Acquisition and Replacement as a Source of Ecological Innovation. *Trends in Microbiology* 25:375–390.

Tanizawa Y, Fujisawa T, Nakamura Y. 2018. DFAST: a flexible prokaryotic genome annotation pipeline for faster genome publication. *Bioinformatics* 34:1037–1039.

Teufel F, Almagro Armenteros JJ, Johansen AR, Gíslason MH, Pihl SI, Tsirigos KD, Winther O, Brunak S, von Heijne G, Nielsen H. 2022. SignalP 6.0 predicts all five types of signal peptides using protein language models. *Nat Biotechnol* 40:1023–1025.

Tinsley MC, Majerus ME. 2007. Small steps or giant leaps for male-killers? Phylogenetic constraints to male-killer host shifts. *BMC Evolutionary Biology* 7:238.

Touchon M, Bernheim A, Rocha EPC. 2016. Genetic and life-history traits associated with the distribution of prophages in bacteria. *The ISME Journal* 10:2744–2754.

Watts T, Haselkorn TS, Moran NA, Markow TA. 2009. Variable Incidence of *Spiroplasma* Infections in Natural Populations of *Drosophila* Species. *PLOS ONE* 4:e5703.

Wernegreen JJ. 2017. In it for the long haul: evolutionary consequences of persistent endosymbiosis. *Current Opinion in Genetics & Development* 47:83–90.

Werren JH. 1998. Wolbachia and Speciation. In: Howard DJ, Berlocher SH, editors. *Endless Forms: Species and Speciation*. Oxford University Press. p. 0. Available from: <https://doi.org/10.1093/oso/9780195109009.003.0018>

Yoshida K, Sanada-Morimura S, Huang S-H, Tokuda M. 2021. Silence of the killers: discovery of male-killing suppression in a rearing strain of the small brown planthopper, *Laodelphax striatellus*. *Proceedings of the Royal Society B: Biological Sciences* 288:20202125.